Improvements in Surface Tension Measurements of Liquid Metals Having Low Capillary Constants by the Constrained Drop Method

Joonho LEE, Akihito KIYOSE,[1,2] Shinichi NAKATSUKA,[2] Masashi NAKAMOTO[2] and Toshihiro TANAKA

Department of Materials Science and Processings, Graduate School of Engineering, Osaka University, 2-1 Yamadaoka, Suita, Osaka 565-0871 Japan. E-mail: juno@mat.eng.osaka-u.ac.jp; tanaka@mat.eng.osaka-u.ac.jp   1) Steelmaking R&D Div., Environment & Process Technology Center, Technical Development Bureau, Nippon Steel Corporation, 20-1 Shintomi, Futtsu, Chiba 293-8511 Japan.   2) Graduate Student, Department of Materials Science and Processings, Graduate School of Engineering, Osaka University, 2-1 Yamadaoka, Suita, Osaka 565-0871 Japan.

Accurate measurements of surface tension of liquid metals having low capillary constants (the ratio between density (ρ) and surface tension (σ), ρ/σ) have been attempted using the constrained drop method. High accuracy of surface tension measurements was obtained by making a large axi-symmetric liquid drop and adopting a developed image capturing system composed of a high-resolution charge-coupled device (CCD) camera, an additional CCD camera to adjust the level of the metal drop and a He–Ne laser.

KEY WORDS: surface tension; liquid metal; Laplace equation; sessile drop method; constrained drop method; capillary constant.

1. Introduction

Surface tension of liquid alloys can be estimated by thermodynamic calculations.[1–8] In the calculations, reliable reference data of the surface tension of the respective pure metal components of the liquid alloy system and its temperature dependence are important.[9] One of the most popular methods in surface tension measurements is the sessile drop method. Recently, from simulations based on Laplace equation, the authors showed that more reliable surface tension values could be obtained as the drop size increases, because the contour of the drop profile is distinguishable clearly to that of slightly changed surface tensions by ±10%.[10] The simulated results were confirmed with measurements of the surface tension of liquid metals having low melting temperatures such as Ga, Sn, Bi, In and Pb by using the constrained drop method with a large axi-symmetric drop in a special crucible as shown in **Fig. 1**(a). In **Fig. 2**, the surface tension measurements of liquid Sn with changing the size of liquid metal drop were plotted as a function of temperature. In order to increase the size of the drop, various crucibles of different sizes (6 mm, 8 mm and 10 mm in diameter) were adopted. The deviation of the sur-
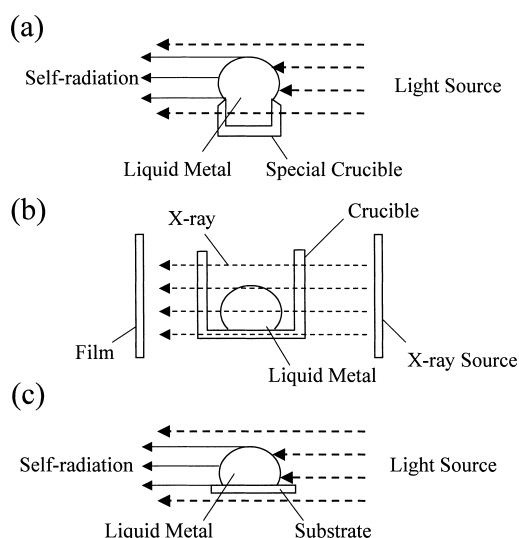

Fig. 1. Various image capturing systems in the sessile drop method: (a) constrained drop method, (b) X-ray radiographic method, (c) traditional sessile drop method.
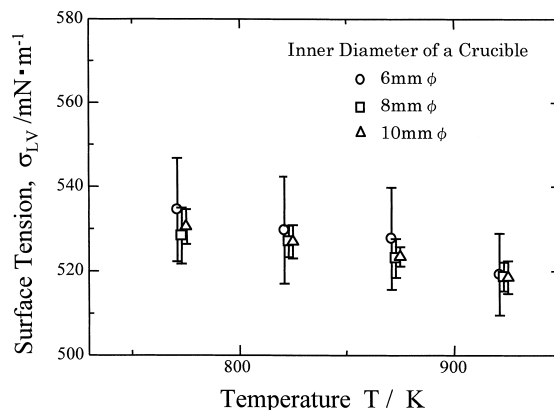

Fig. 2. Surface tension of liquid Sn with crucibles of various sizes.[10]

Table 1. Capillary constant of various metals at their melting temperatures.

Element	Bi	In	Sn	Ga	Ag	Cu	Fe	Co
Density, ρ / 10^{-3} kg/m^3 [24]	10.05	7.03	6.98	6.10	9.33	8.00	7.03	7.75
Surface Tension, σ / N/m [24]	0.378	0.556	0.560	0.718	0.966	1.303	1.872	1.873
Capillary Constant, C.C. / 10^{-3} kg/Nm^2	26.59	12.64	12.46	8.50	9.66	6.14	3.76	4.14

face tension measurements reduced less than ±1% with the crucibles of 8 mm and 10 mm in diameter. Originally, this founding had been reported by Ukraine researchers. Naidich *et al.*[11] early reported that the accuracy of surface tension measurements increased with applying the modified sessile drop method making a large axi-symmetric drop in a crucible. Recently, Lin *et al.*[12] and Morita *et al.*[13] reported that the accuracy of the surface tension measurements by the pendant drop method also increased with increasing the drop size. But these researches have focused only on the size itself. In our previous work, from the simulations the change in the surface profile due to the uncertainty in the surface tension was found to be dependent upon the capillary constant (=C.C.), the ratio of ρ (density)/σ (surface tension), *i.e.*, a liquid metal having the lower capillary constant has a tendency to form a more spherical shape,[14] of which the contour is more indistinguishable to that of the slightly changed surface tension. Thus, in order to measure the surface tension of liquid metals having low capillary constants by the sessile drop method, we should be careful to acquire a clear surface profile of the liquid drop. Since a metal of a low capillary constant usually has a high melting temperature, the surface tension measurements are often conducted with the X-ray radiographic images[15–18] or the self-radiant images[19–23] (Figs. 1(b) and 1(c)). However, if the X-ray radiographic image or the self-radiant image is applied, it can be difficult to obtain the accurate information of the surface profile, which is most important in the analysis of the surface tension, because of the shallow penetration length of the X-ray beam through the surface of the sessile drop or the smooth change in the brightness across the metal surface, respectively. As a result, the experimental scattering of reported measurements has been more than ±3–12%. In the present work, liquid Ag, Cu, Fe and Co, which have much lower capillary constants and higher melting temperatures rather than those metals in our previous work, were examined to determine the surface tension experimentally by the constrained drop method with large drops stabilized in a special crucible. (**Table 1** shows C.C. of various metals at their melting temperatures.) This paper presents the developments in measurements of the surface tension of liquid metals having such low capillary constants with high precision by using the constrained drop method.

2. Simulation of the Shape of a Sessile Drop

The profile of a liquid drop is drawn from Laplace equation.
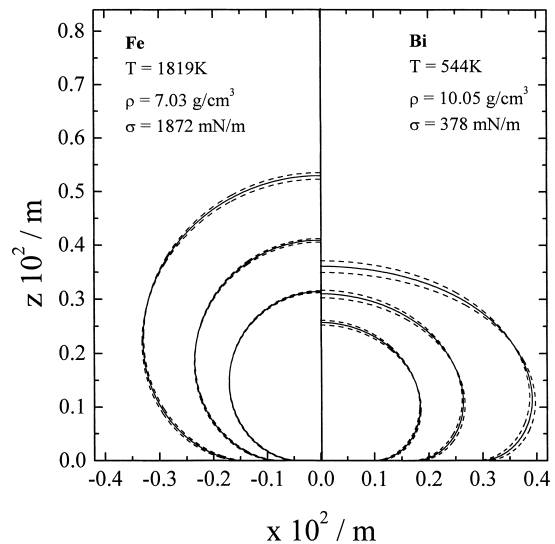
Fig. 3. Change in droplet shape with size for Fe and Bi (V=1.99, 4.98, 12.94×10^{-8} m^3). Dashed lines show the shape with varying the surface tension by 10%. Contact angle was assumed as 180°.

$$\left(\frac{1}{R_1} + \frac{\sin\phi}{x}\right) = \frac{2}{R_o} + \frac{z}{\alpha^2} \quad \text{...................(1)}$$

$$\alpha^2 = \sigma/\Delta\rho g \quad \text{................................(2)}$$

where σ, R_1, R_o, ϕ, $\Delta\rho$, g, x and z denote the surface tension, the curvature radius at a point of interest, the curvature radius at the apex, the turning angle, the difference in densities between the drop and the surrounding phase (in this case, the density of liquid metals), the gravitational constant, the horizontal position and the vertical position of the point from the apex. The details can be found in the literatures.[9,10,16,19]

In **Fig. 3**, the comparison is shown of the simulated results of the surface profile between liquid Bi (C.C.=26.59) and Fe (C.C.=3.76) at their melting temperatures. In the previous contribution,[10] with a fixed height, the profiles of liquid metal drops were simulated when the surface tension value changes by ±10%. In a real case, however, it is more reasonable to compare the profile of the liquid drop at a constant volume, especially for the metals having low C.C. values. In the present work, therefore, the profiles of drops for liquid Bi and Fe have been drawn with fixing the volume of the drops. The surface tension and the density were quoted from ref. 24. The volume of the liquid drops was assumed as 1.99, 4.98 and 12.94×10^{-8} m^3. As convinced in our previous work, with increasing the size of the liquid drop, its surface profile (solid lines) becomes more distinguishable to that plotted by changing the surface tension values by ±10% (dashed lines). It is also found that the surface profile of Fe is more indistinguishable than that of Bi at the same volume. Accordingly, the same accuracy in the surface tension of the liquid metals having lower C.C. such as Fe would be obtained with much larger samples than those of higher C.C. such as Bi. To get a clear surface image of a much larger drop is practically difficult. Hence, in the present work, we attempted to get a much clearer image by adopting a high-resolution CCD camera with a
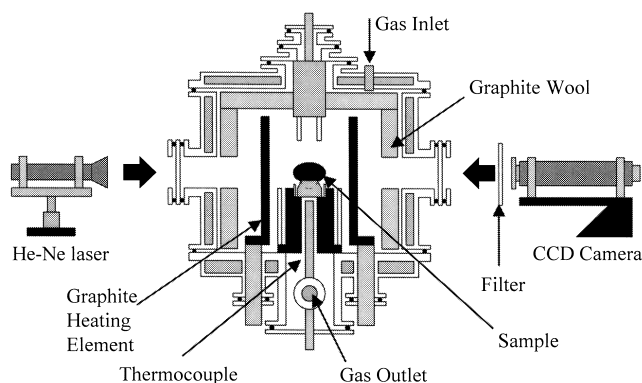
Fig. 4. Schematic illustration of experimental apparatus for the constrained drop technique.
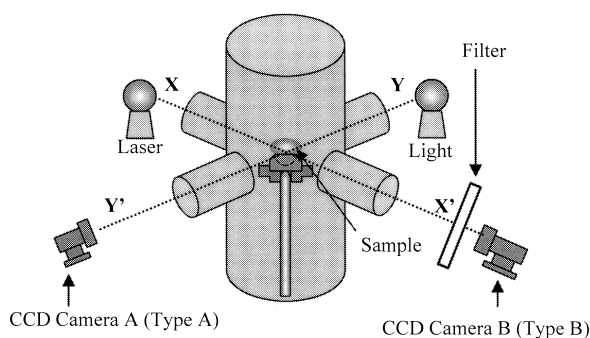
He–Ne laser.

Fig. 5. Schematic illustration of the arrangement of the CCD cameras. The camera A is for the investigation of the inclination of the sample, and the camera B is for the investigation of the contour of the sample drop to calculate the surface tension.

3. Experimental

3.1. Apparatus and Materials

In the present work, the surface tension was measured by using a graphite-heating-element furnace ($T_{Max.}=1\,973\,K$) with a high-resolution CCD camera ($1\,636\times1\,236$ pixels) as shown in **Figs. 4** and **5**. A pixel corresponds to $8.824\,\mu m$ with the CCD camera. A He–Ne laser rays ($\lambda=632.8\,nm$) along the X–X′ axis (the investigating direction) was used to capture a much clearer image profile of the liquid metal drop. In order to investigate the level for the X–X′ direction, another CCD camera along the Y–Y′ axis was applied. It was possible to level a graphite stage by adjusting three poles sustaining the furnace. The temperature was measured with a Pt–30%Rh/Pt–6%Rh thermocouple, which was set directly under the crucible. The temperature was controlled manually within $\pm1\,K$. High purity metals (Ag: >99.99 mass%, Cu: >99.998 mass%, Fe: >99.998 mass% and Co: >99.998 mass%) were used. Graphite and alumina crucibles were used in the experiments with the samples of Ag and Cu, and those of Fe and Co, respectively, because carbon may dissolve in liquid Fe and Co, changing the surface tension values.[20,25] During experiments, the reaction furnace was maintained in a strong reduction atmosphere by flowing 10%H$_2$–Ar gas mixture, which was purified using columns of silica-gel, ascarite, cold-trap (dry ice–methanol) and Mg chips at 773 K to eliminate reported contaminants, essentially H$_2$O, CO, CO$_2$ and O$_2$, causing adsorption of oxygen to decrease the surface tension.
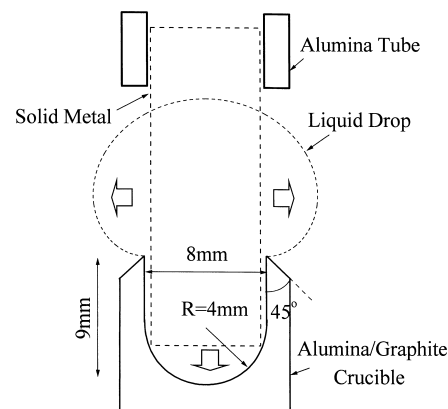

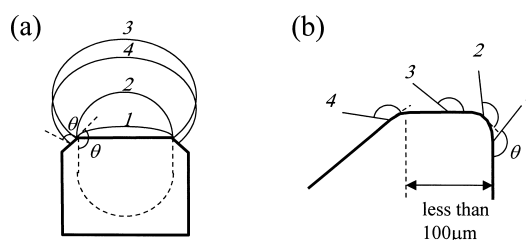**Fig. 6.** Schematic diagram of making a liquid drop in a crucible.

Fig. 7. Schematic diagram of (a) macroscopic and (b) microscopic triple points at the edge of the crucible.

Chemical analysis after experiments showed that the oxygen content in Fe was less than 10 ppmw, which might not affect the surface tension values. It is considered that oxygen contamination for Ag, Cu and Co in the same atmosphere is much smaller.

3.2. Procedure

The sample metal was prepared as cylindrical pieces of 5–7 mm in diameter, and used after removing surface contaminants with a grit paper and washed in acetone using an ultrasonic cleaner. In order to make the melted sample settled stably in the crucible, the sample was sustained by an alumina tube as shown in **Fig. 6**. After the sample assembly was placed at the center of the furnace, the reaction furnace was sealed and evacuated, and then the purified 10%H$_2$–Ar gas mixture was introduced for 12 h. Then, the furnace was heated to the experimental temperature in 2–2.5 h. When the sample was melted, the alumina tube sustaining the sample was removed (Fig. 6), and then the measurements were started. **Figure 7** shows a schematic illustration of the triple point at the crucible tip. The tip of the crucible has a flat surface of less than $100\,\mu m$ wide. At the edge of the crucible tip, the true local contact angle (θ) remains constant, whereas the apparent contact angle varies between $\theta-90$ deg and $\theta+45$ deg. The optimum condition of measurements is the case of line 3, where the local contact angle and the apparent contact angle are the same. The shape of a large drop was investigated by the high-resolution CCD camera. Then, the surface tension of the liquid metal was calculated with a computer program.[26] The whole image processing sequences are shown in **Fig. 8**. In **Table 2**, a typical set of data of the surface profile in pixels is given. The displacement of the center from the mean value shows the distortion of the shape of liquid drop. As
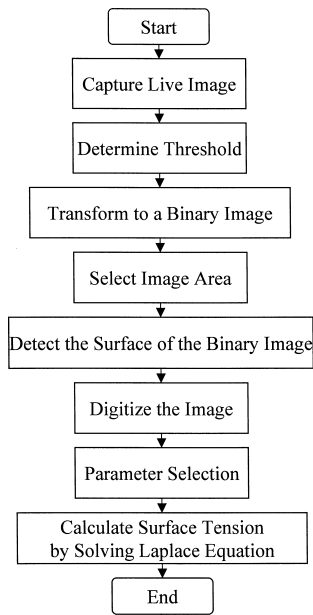
Fig. 8. The sequence of the image processing for the analysis of the surface tension.

Table 2. Typical set of data points selected from the surface profile of liquid Ag in pixels.

No.	left	right	center	displacement	height
1	146	1266	706	2	197
2	136	1277	706.5	1.5	241
3	138	1276	707	1	321
4	164	1253	708.5	-0.5	403
5	211	1207	709	-1	481
6	299	1119	709	-1	568
7	441	979	710	-2	646
Mean			708		

the height increases from 197 to 646 pixel, the displacement changes from -2 to $+2$. From this, we may consider that the distortion of the image may be caused by the slight inclination of the crucible. The inclination of this sample is only 0.5 deg. ($=\tan^{-1}(4/450)$). In addition, the apparent contact angle of the right and the left are, respectively, 135.0 and 134.6 deg., which are coincident with the value obtained from the computer program, 134.2 deg. Accordingly, it can be concluded that the present method provides very accurate axi-symmetric surface profile of a large liquid drop.

3.3. Experimental Accuracy

In the present work, the dependence of errors upon the CCD's resolution was simulated for Fe, which has the lowest C.C. in this work, with two different CCD cameras; Type A (512×512 pixel) and Type B (1 636×1 236 pixel). When the Type A was employed, the maximum error caused for Fe by ± 1 pixel was calculated to be, 2.4%, and that by ± 3 pixels was 6.4%. However, when the Type B was employed, those for Fe by ± 1 and ± 3 pixels reduced to 1.1% and 2.0%, respectively. Accordingly, the maximum experimental error of the present work is less than $\pm 2\%$ at most. (The experimental error decreases with increasing C.C.)
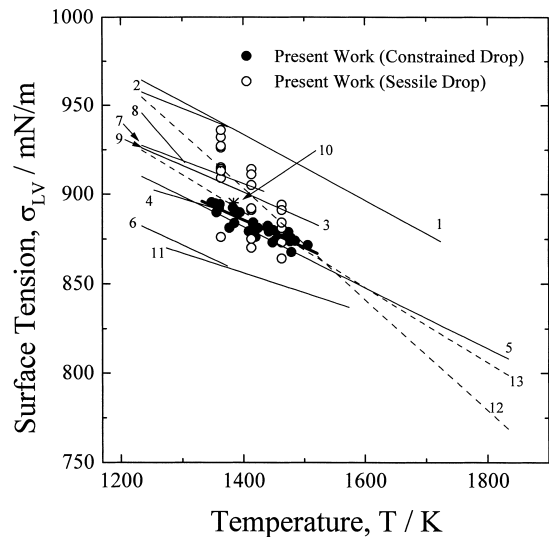

Fig. 9. Surface tension of liquid Ag as a function of temperature. (1: Kasama,[27] 2: Rhee,[28] 3: Brunet,[29] 4: Bernard,[30] 5: Nogi,[31] 6: Sangiorgi,[32] 7: Krause,[33] 8: Kingery,[34] 9: Joud,[35] 10: Sebo,[36] 11: Pawlek,[37] 12: Keene (suggested),[9] 13: Keene (mean value of the reported measurements)[9])

4. Results and Discussion

4.1. Surface Tension of Liquid Ag

Initially, the technique was applied to a well-known and well-determined standard metal at high temperatures: liquid Ag. In **Fig. 9**, the value of surface tension of liquid Ag is shown with temperature. Solid circles and open circles are measurements of the present work using the constrained drop and the traditional sessile drop methods, respectively. Both data are within the scatter of reported values (solid lines[9,27-37] in Fig. 8: Every data referred in this contribution (Figs. 9, 11–13) was only those measured by the traditional sessile drop method.), but the deviation of experimental results using the constrained drop method is clearly smaller than those using the traditional sessile drop method. In Fig. 9, the "suggested" σ–T relation (dashed line) and the mean value of reported measurements after Keene[9] are also drawn for comparison. The temperature dependence of the surface tension in the present work is very closer to that after Nogi et al.[31] and the mean value of reported measurements after Keene than the "suggested" relation after Keene. Keene considered that the major error source in the surface tension measurements is the adsorption of surface active elements such as oxygen and sulfur on the surface of liquid metals, so that he decided the "suggested" relation based only upon the reported data having higher surface tensions. Recently, Jimbo and Cramb[16] pointed out that the surface tension of liquid metal could be highly estimated by about 13% due to the inclination of the substrate for the direction of the investigation (X–X' direction in Fig. 5). In the measurements using the large drop, we adopted a CCD camera to investigate and adjust the level of the liquid metal along the Y–Y' axis. Thus, it is considered that this error source was avoided enough by confirming the level with the program developed by Jimbo and Cramb.[16] The temperature dependence of the surface tension of liquid Ag is given by Eq. (3).
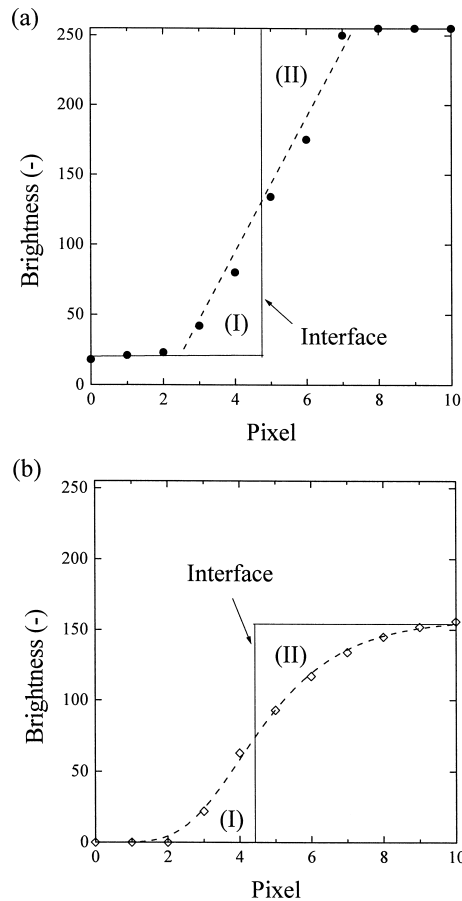
Fig. 10. The brightness change at the interface between the sessile drop and the surroundings for the images (a) with and (b) without laser. The interface was determined as (I) and (II) have the same area.

$$\sigma_{Ag} = 911 - 0.153 \times (T - 1\,234) \text{ (mN/m)}$$
$$(1\,348 \leq T \leq 1\,506 \text{ K}) \dots\dots\dots\dots\dots\dots(3)$$

4.2. Effect of Using Laser on Experimental Accuracy

In surface tension measurements below about 1 473 K, a halogen lamp can be used as the light source making shadow image of the sessile drop. As temperature increases, however, the intensity of the self-radiation of the liquid metal drop increases, so that many researchers captured the image of the sessile drop using the self-radiation.[19–23] However, as addressed before, to get a clear image of the drop profile, the interface between the sessile drop and the surroundings atmosphere should be clearly distinguished. In order to get a sharp threshold of the sessile drop image, a He–Ne laser was used as the light source in the present work. Due to strong intensity of the He–Ne laser, a special light filter as shown in Fig. 4 was applied. In **Fig. 10**, the brightness changes at the interface between the sessile drop and the surroundings (a) with laser and (b) without laser are given. It is found that the brightness at the interface for the image obtained by using a He–Ne laser changes linearly, whereas that by using a self-radiant image shows a smooth curve. As a result, the interface obtained for different positions by using the self-radiant image yields different threshold intensities, which made it difficult to decide the whole interface profile with a constant threshold value. In order to understand the effect of the slow change of the brightness

Table 3. The simulated results on the deviation in measuring surface tensions by changing the threshold value of a drop image.

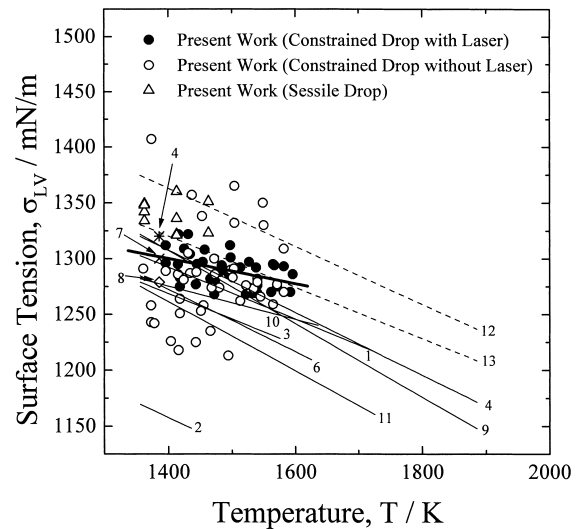| Change Brightness from the Threshold	+5	+10	+20	-5	-10	-20
With Laser / %	0.25	0.36	0.36	0.30	0.35	0.41
Self-radiant / %	0.46	0.55	1.10	0.56	0.61	1.25

Fig. 11. Surface tension of liquid Cu as a function of temperature. (1: Kasama,[27] 2: Rhee,[28] 3: Pawlek,[37] 4: Gallios,[38] 5: Nogi,[31] 6: Gans,[37] 7: Sebo,[36] 8: Joud,[35] 9: Jakobsson,[40] 10: Lang,[41] 11: Allen,[42] 12: Keene (suggested),[9] 13: Keene (mean value of the reported measurements)[9])

in the self-radiant image, the difference in the surface tension values by intentional changes in the brightness value by ±5, ±10 and ±20 from the threshold value was computed. Calculated deviations are shown in **Table 3**. With a laser image, the change in the surface tension is less than 0.41%, whereas 1.3% with a self-radiant image. In **Fig. 11**, the surface tension measurements of liquid Cu with and without laser are plotted. Solid circles and open circles represent data with and without laser, respectively. The experimental scatter without laser is within 8.0%, but that with laser decreases to 2.0%. The temperature dependence of the surface tension of liquid Cu with laser is given by Eq. (4).

$$\sigma_{Cu} = 1\,305 - 0.113 \times (T - 1\,356) \text{ (mN/m)}$$
$$(1\,391 \leq T \leq 1\,596 \text{ K}) \dots\dots\dots\dots\dots\dots(4)$$

The absolute value of the temperature dependence is slightly smaller than the reported values. The surface tension obtained in the present work show much closer values to the mean values of the reported values than the suggested ones after Keene.[9]

4.3. Surface Tension of Liquid Fe and Co

Figures 12 and **13** show the experimental results of the surface tension of liquid Fe and Co, respectively. When we measured the surface tension of liquid Fe with the traditional sessile drop method (open circles in Fig. 12), the experimental scatter is within ±6.8%. The measurements by using the constrained drop method decreased the scatter to
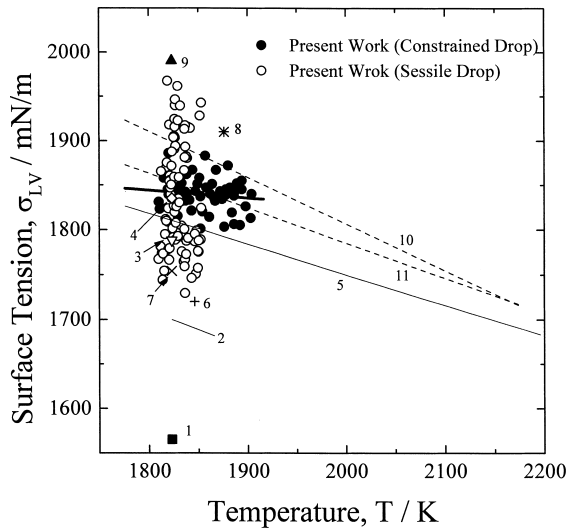
Fig. 12. Surface tension of liquid Fe as a function of temperature. (1: Kingery,[34] 2: Allan,[42] 3: Kozakevitch,[43] 4: Kozakevitch,[44] 5: Krinochkin,[45] 6: Halden,[46] 7: Dyson,[47] 8: Ogino,[48] 9: Zhu,[23] 10: Keene (suggested),[9] 11: Keene (mean value of the reported measurements)[9])
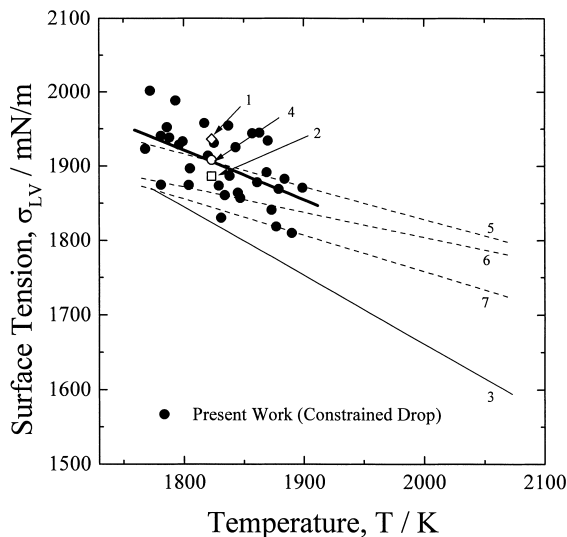

Fig. 13. Surface tension of liquid Co as a function of temperature. (1: Kozakevitch,[44] 2: Kozakevitch,[43] 3: Allen,[42] 4: Wang,[25] 5: Keene (suggested),[9] 6: Keene (mean value of the reported measurements),[9] 7: Iida (suggested)[24])

within ±2.4. The experimental scatter of the surface tension of liquid Co was within ±3.0%. The temperature dependence of the surface tension of liquid Fe and Co obtained in the present work is given as follows:

$$\sigma_{Fe} = 1\,843 - 0.186 \times (T - 1\,808)\,(\text{mN/m})$$

$$(1\,811 \leq T \leq 1\,904\,\text{K}) \quad\text{........................(5)}$$

$$\sigma_{Co} = 1\,944 - 0.666 \times (T - 1\,765)\,(\text{mN/m})$$

$$(1\,768 \leq T \leq 1\,899\,\text{K}) \quad\text{........................(6)}$$

The temperature dependence of the surface tension of liquid Cu, Fe and Co shows relatively smaller or higher values than the suggested values.

5. Conclusions

(1) The effects of the size and the capillary constant of a drop on the accuracy of measuring the surface tension of liquid metals were simulated using Laplace equation. It was found that the accuracy of the surface tension would increase with increasing the size and capillary constant.

(2) By adopting a high-resolution CCD camera, a He–Ne laser and a CCD camera to adjust the level of the liquid metal drop, the experimental accuracy of measurements of the surface tension increased.

(3) The surface tension of liquid Ag, Cu, Fe and Co was determined within experimental scatter of less than ±3%. The surface tensions of liquid Ag, Cu, Fe and Co could be expressed by $\sigma_{Ag} = 911 - 0.153 \times (T - 1\,234)$, $(1\,348 \leq T \leq 1\,506\,\text{K})$, $\sigma_{Cu} = 1\,305 - 0.113 \times (T - 1\,356)$, $(1\,391 \leq T \leq 1\,596\,\text{K})$, $\sigma_{Fe} = 1\,843 - 0.086 \times (T - 1\,808)$, $(1\,811 \leq T \leq 1\,904\,\text{K})$, and $\sigma_{Co} = 1\,944 - 0.666 \times (T - 1\,765)$, $(1\,768 \leq T \leq 1\,899\,\text{K})$, respectively.

REFERENCES

1) R. Speiser, D. R. Poirier and K. Yeum: *Scr. Metall.*, **21** (1987), 687.
2) K. S. Yeum, R. Speiser and D. R. Poirier: *Metall. Trans. B*, **20B** (1989), 693.
3) T. Tanaka and T. Iida: *Steel Res.*, **65** (1994), 21.
4) T. Tanaka, K. Hack, T. Iida and S. Hara: *Z. Metallkd.*, **87** (1996), 380.
5) T. Tanaka, K. Hack and S. Hara: *MRS Bulletin*, **24** (1999), 45.
6) T. Tanaka, K. Hack and S. Hara: *Calphad*, **24** (2000), 465.
7) Z. Qiao, L. Yan, Z. Cao and Y. Xie: *J. Alloys Comp.*, **325** (2001), 180.
8) R. Novakovic, E. Ricci, M. L. Muolo, D. Giuranno and A. Passerone: *Intermetallics*, **11** (2003), 1301.
9) B. J. Keene: *Int. Mater. Rev.*, **38** (1993), 157.
10) T. Tanaka, M. Nakamoto, R. Oguni, J. Lee and S. Hara: *Z. Metallkd.*, **95** (2004), 818.
11) Yu. V. Naidich and V. N. Eremenko: *Fiz. Met. Metalloved.*, **11** (1961), 883.
12) S. Y. Lin, L. J. Chen, J. W. Xyu and W. J. Wang: *Langmuir*, **11** (1995), 4159.
13) A. T. Morita, D. J. Carastan and N. R. Demarquette: *Colloid Polym. Sci.*, **280** (2002), 857.
14) J. Lee, K. Morita and T. Tanaka: *Mater. Trans.*, **44** (2003), 2659.
15) K. Ogino, S. Hara, T. Miwa and S. Kimoto: *Tetsu-to-Hagané*, **65** (1979), 30.
16) I. Jimbo and A. W. Cramb: *ISIJ Int.*, **32** (1992), 26.
17) A. Sharan and A. W. Cramb: *Metall. Mater. Trans. B*, **28B** (1997), 465.
18) M. Divakar, J. P. Hajra, A. Jakobsson and S. Seetharaman: *Metall. Mater. Trans. B*, **31B** (2000), 267.
19) J. Lee and K. Morita: *ISIJ Int.*, **42** (2002), 588.
20) J. Lee and K. Morita: *Steel Res.*, **73** (2002), 367.
21) Y. Chung, A.W. Cramb: *Steel Res.*, **70** (1999), 325.
22) K. Mukai and Z. Yuan: *Mater. Trans. JIM*, **41** (2000), 331.
23) J. Zhu and K. Mukai: *ISIJ. Int.*, **38** (1998), 1039.
24) T. Iida and R. I. L. Guthrie: The Physical Properties of Liquid Metals, Clarendon Press, Oxford, (1988), 71, 134.
25) J. Wang, H. Wang and M. Bian: *Z. Phys. Chem.*, **156** (1988), 599.
26) A. S. Krylov, A. V. Vvedensky, A. M. Katsnelson and A. E. Tugovikov: *J. Non-Cryst. Solids*, **156–158** (1993), 845.
27) A. Kasama, T. Iida and Z. Morita: *J. Jpn. Inst. Met.*, **40** (1976), 1030.
28) S. K. Rhee: *J. Am. Ceram. Soc.*, **53** (1970), 639.
29) M. Brunet, J. C. Joud, N. Eustathopoulos and P. Desre: *J. Less-Common. Met.*, **51** (1977), 69.
30) G. Bernard and C. H. P. Lupis: *Metall. Trans.*, **2** (1971), 555.
31) K. Nogi, K. Oishi and K. Ogino: *Mater. Trans. JIM*, **30** (1989), 137.
32) R. Sangiorgi, M. L. Muolo and A. Passerone: *Acta Metall.*, **30** (1982), 1597.
33) W. Krause, F. Sauerwald and M. Michalke: *Z. Arong. Chem.*, **18**

(1929), 353.

34) W. D. Kingery and M. Humenik, Jr.: *J. Phys. Chem.*, **57** (1953), 359.

35) J.-C. Joud, N. Eustathopoulos and A. B. P. Desré: *J. Chim. Phys.*, **70** (1973), 1290.

36) P. Sebo, B. Gallios and C. H. P. Lupis: *Metall. Trans. B*, **8B** (1977), 691.

37) F. Pawlek, W. Thielsch and W. Wuth: *Metall.*, **15** (1961), 1076.

38) B. Gallios and C. H. P. Lupis: *Metall. Trans. B*, **12B** (1981), 549.

39) W. Gans, F. Pawlek and A. Röpenack: *Z. Metallkd.*, **54** (1963), 147.

40) A. Jakobsson, N. N. Viswanathan, D. Sichen and S. Seetharaman: *Metall. Mater. B*, **31B** (2000), 973.

41) G. Lang, P. Laty, J.-C. Joud and P. Desré: *Z. Metallkd.*, **68** (1977), 113.

42) B. C. Allan and W. D. Kingery: *Trans. AIME*, **215** (1959), 30.

43) P. Kozakevitch and G. Urbain: *Acad. Sci.*, **13** (1961) 2229.

44) P. Kozakevitch and G. Urbain: *J. Iron Steel Inst.*, **179** (1957), 167.

45) E. V. Krinochkin, K. T. Kurochkin and P. V. Umrikhin: *Izv. Akad. Nauk. SSSR. Met.*, No. 5, (1971), 67.

46) F. A. Halden and W. D. Kingery: *J. Phys. Chem.* **59** (1955), 557.

47) B. F. Dyson: *Trans. AIME*, **227** (1963), 1098.

48) K. Ogino, K. Nogi and C. Hosoi: *Tetsu-to-Hagané*, **69** (1983), 1989.